Dufour and Soret effects on heat and mass transfer in a micropolar fluid in a horizontal channel

FAIZ AWAD and PRECIOUS SIBANDA
University of KwaZulu-Natal
School of Mathematical Sciences
Private Bag X01, Scottsville
Pietermaritzburg 3209
SOUTH AFRICA
sibandap@ukzn.ac.za

Abstract: The problem of free convection of heat and mass in micropolar fluid in a channel subject to cross diffusion (namely the Soret and Dufour effects) is presented. The effect of small and large Peclet numbers on the temperature and concentration profiles is determined while the effects of various parameters such as the Reynolds number, the coupling parameter and the spin gradient viscosity parameter on the fluid properties are determined and shown graphically. The study uses the homotopy analysis method to find approximate analytical series solutions for the governing system of nonlinear differential equations. The analytical results are validated using the Matlab bvp4c numerical routine.

Key–Words: Micropolar fluid, heat transfer, mass transfer, Peclet numbers, homotopy analysis method

1 Introduction

The concept of a micropolar fluid derives from the need to model the flow of fluids that contain rotating micro-constituents (see Eringen [1, 2]). The usual Navier-Stokes equations cannot adequately describe the motion of such fluids. Examples of flows that have been adequately explained using the concept of micropolar fluids include the flow of colloidal solutions [3], liquid crystals [4], polymeric fluids and blood [5] as well as fluids with additives, [6].

The field of micropolar fluids is very rich in literature, with various aspects of the problem having been investigated. Examples include Peddieson and McNitt [7], Gorla [8], Rees and Bassom [9] who investigated the flow of a micropolar fluid over a flat plate and Kelson and Desseaux [10], who studied flow of micropolar fluids on stretching surfaces Heat and mass transfer is important in many industrial and technological processes. In manufacturing and metallurgical processes, heat and mass transfer occur simultaneously. Heat transfer problems in micropolar fluids have been investigated by, among others, Perdikis and Raptis [11] and Raptis [12] who also studied the effects of heat radiation. The effect of radiation and suction/injection was studied by El-Arabawy [13] while the effects of radiation in a porous medium were studied by Abo-Eldahab and Ghonaim [14]. Hassanien et al. [15] studied the effect of a constant heat flux in a porous medium while Aissa and Modammadein [16] and Soundalgekar and Takhar [17] studied heat transfer past a continuously moving flat surface.

In Mohammadein and Gorla [18] micropolar flow along a stretching sheet with prescribed wall heat flux, viscous dissipation and internal heat generation was investigated. Rahman and Sultana [19] investigated the problem of radiative heat transfer, viscous dissipation and joule heating in a micropolar fluid flow past a uniformly heated vertical permeable surface. The governing equations were solved using a shooting method. Kim and Lee [20] investigated the oscillatory flow of a micropolar fluid over a vertical porous plate while Sharma and Gupta [21] studied the effects of porous medium permeability and thermal convection in micropolar fluids. Khader et al. [6] investigated the problem of steady, laminar boundary-layer flow of a viscous, micropolar fluid past a vertical uniformly stretched permeable plate with heat generating or absorption. They used the finite-difference method to solve the governing nonlinear equations. Rahman and Sultana [19] used the Nachtsheim-Swigert shooting iteration technique to investigate the problem of radiative heat transfer flow of micropolar fluid past a vertical permeable flat plate embedded in a porous medium with varying surface heat flux. Using the Keller-box method, Roslinda et al. [22] solved the problem of unsteady boundary layer flow of a micropolar fluid over a stretching sheet. The equations governing the flow of a micropolar fluid flow with uniform suction/blowing and heat generation were solved by Ziabakhsh et al. [23] using the homotopy analysis method.

Muthucumaraswamy and Ganesan [24] investigated the effect of a chemical reaction and injection on the flow characteristics of an unsteady upward motion of an isothermal plate. Perdikis and Raptis [11] analyzed the effect of a chemical reaction on an electrically conducting viscous fluid flow over a nonlinearly stretching semi-infinite sheet in the presence of a constant magnetic. Ibrahim et al. [25] analyzed the effects of a chemical reaction and radiation absorption on the unsteady MHD free convection flow past a semi-infinite vertical permeable plate with heat sources and suction. The influence of a chemical reaction and thermal radiation on the heat and mass transfer in MHD micropolar flow over a vertical moving plate in a porous medium with heat generation was studied by Mohammed and Abo-Dahab [26]. Ziabakhsh and Domairry [27] used the homotopy analysis method to solve the problem of mass transfer in a micropolar fluid in a porous channel.

The aim of this study is to investigate the problem of combined heat and mass transfer in a micropolar fluid. Most earlier studies, with a few exceptions such as Mohamed and Abo-Dahab [26] and Sajid et al. [28] do not consider the effect of a chemical reaction.

Combined heat and mass transfer driven by buoyancy due to temperature and concentration variations has many possible engineering applications, for example, the migration of moisture through air contained in fibrous insulations and grain storage systems, the dispersion of chemical contaminants through water-saturated soil, and the underground disposal of nuclear wastes, see Narayana and Sibanda [29]. In recent years a large number of studies dealing with the effects of Dufour and Soret parameters on heat and mass transfer problems on Newtonian and viscoelastic fluids have appeared. These effects are considered as second order phenomena and have often been neglected in heat and mass transfer processes, see Mojtabi and Charrier-Mojtabi [30]. Recent examples of studies that investigated Dufour and Soret effects include those of Postelnicu [31] who studied the Dufour and Soret effects on the simultaneous heat and mass transfer from a vertical plate embedded in an electrically conducting fluid and Alam et al. [32] who studied the Dufour and Soret effects on heat and mass transfer for flow past a semi-infinite vertical plate. Alam and Rahman [33] studied the effects of the Dufour and Soret parameters on mixed convection in a flow past a vertical plate embedded in a porous medium. Li et al. [34] considered thermal-diffusion and diffusion-thermo effects on the characteristics of heat and mass transfer in a strongly endothermic chemical in a porous medium. Gaikwad et al. [35] investigated the onset of double diffusive convection in a two-component couple stress fluid layer with Soret and Dufour effects using both linear and nonlinear stability analysis. An extensive literature review on this subject can be found in recent books by Nield and Bejan [36] and by Pop and Ingham [37] and the references therein.

2 Mathematical formulation

We consider the steady laminar flow of a micropolar fluid along a two-dimensional channel with porous walls through which fluid is uniformly injected or removed with speed v_0. The lower channel wall has a solute concentration C_1 and temperature T_1 while the upper wall has solute concentration C_2 and temperature T_2. Using cartesian coordinates, the channel walls are parallel to the x-axis and located at $y = \pm h$ where $2h$ is the channel width. The relevant equations governing the flow are

$$\frac{\partial u}{\partial x} + \frac{\partial v}{\partial y} = 0, \tag{1}$$

$$u\frac{\partial u}{\partial x} + v\frac{\partial u}{\partial y} = -\frac{1}{\rho}\frac{\partial p}{\partial x} + \left(\frac{\mu + k}{\rho}\right)\left[\frac{\partial^2 u}{\partial x^2} + \frac{\partial^2 u}{\partial y^2}\right] + \frac{k}{\rho}\frac{\partial N}{\partial y}, \tag{2}$$

$$u\frac{\partial v}{\partial x} + v\frac{\partial v}{\partial y} = -\frac{1}{\rho}\frac{\partial p}{\partial y} + \left(\frac{\mu + k}{\rho}\right)\left[\frac{\partial^2 v}{\partial x^2} + \frac{\partial^2 v}{\partial y^2}\right] - \frac{k}{\rho}\frac{\partial N}{\partial x}, \tag{3}$$

$$u\frac{\partial N}{\partial x} + v\frac{\partial N}{\partial y} = -\frac{k}{\rho j}\left(2N + \frac{\partial u}{\partial y} + \frac{\partial v}{\partial x}\right) + \frac{\nu_s}{\rho j}\left(\frac{\partial^2 N}{\partial x^2} + \frac{\partial^2 N}{\partial y^2}\right), \tag{4}$$

$$u\frac{\partial T}{\partial x} + v\frac{\partial T}{\partial y} = \frac{k_1}{\rho c_p}\frac{\partial^2 T}{\partial y^2} + \frac{D_m k_T}{c_s c_p}\frac{\partial^2 C}{\partial y^2}, \tag{5}$$

$$u\frac{\partial C}{\partial x} + v\frac{\partial C}{\partial y} = D^*\frac{\partial^2 C}{\partial y^2} + \frac{D_m k_T}{T_m}\frac{\partial^2 T}{\partial y^2}, \tag{6}$$

where u and v are the velocity components along the x- and y- axes respectively, ρ is the fluid density, μ is the dynamic viscosity, N is the angular or micro rotation velocity, p is the fluid pressure, T and c_p are the fluid temperature and specific heat at constant pressure respectively, C is the species concentration, k_1 and D^* are the thermal conductivity and molecular diffusivity respectively, j is the micro-inertia density, k is a material parameter, $\nu_s = (\mu + k/2)j$ is the micro rotation viscosity, k_T, c_s and T_m are the thermal-diffusion ratio, the concentration susceptibility and the fluid mean temperature, and D_m is the effective mass diffusivity rate.

The appropriate boundary conditions are

$$y = -h: \; v = u = 0, \; N = -s\frac{\partial u}{\partial y}$$
$$y = \;\; h: \; v = 0, \, u = \frac{v_0 x}{h}, \; N = \frac{v_0 x}{h^2}, \quad (7)$$

where s is a boundary parameter and indicates the degree to which the microelements are free to rotate near the channel walls. The case $s = 0$ represents concentrated particle flows in which microelements close to the wall are unable to rotate. Other interesting particular cases that have been considered in the literature include $s = 1/2$ which represents weak concentrations and the vanishing of the antisymmetric part of the stress tensor and $s = 1$ which represents turbulent flow. We introduce the following dimensionless variables

$$\eta = \frac{y}{h}, \; \psi = -v_0 x f(\eta), \; N = \frac{v_0 x}{h^2} g(\eta),$$
$$\theta(\eta) = \frac{T - T_2}{T_1 - T_2}, \; \phi(\eta) = \frac{C - C_2}{C_1 - C_2} \quad (8)$$

where $T_2 = T_1 - Ax$, $C_2 = C_1 - Bx$ with A and B constant. The stream function is defined in the usual way;

$$u = \frac{\partial \psi}{\partial y} \quad \text{and} \quad v = -\frac{\partial \psi}{\partial x}.$$

Equations (1) - (7) reduce to the coupled system of nonlinear differential equations

$$\lambda_1 f^{IV} - N_1 g'' - Re(ff''' - f'f'') = 0, \; (9)$$
$$N_2 g'' + N_1(f'' - 2g) - N_3 Re(fg' - f'g) = 0, \; (10)$$
$$\theta'' + D_f \phi'' + Pe_h f'\theta - Pe_h f\theta' = 0, \quad (11)$$
$$\phi'' + S_r \theta'' + Pe_m f'\phi - Pe_m f\phi' = 0, \quad (12)$$

where $\lambda_1 = 1 + N_1$ and subject to the boundary conditions

$$\eta = -1 : f = f' = g = 0, \; \theta = \phi = 1, \; (13)$$
$$\eta = 1 : f = \theta = \phi = 0, f' = -1, g = 1. (14)$$

The parameters of primary interest are the Soret parameter S_r, the Dufour parameter D_f, the Peclet numbers for the diffusion of heat Pe_h and mass Pe_m respectively, the Reynolds number Re where for suction $Re > 0$ and for injection $Re < 0$ and the Grashof number Gr given by

$$S_r = \frac{k_2}{D^*}\frac{T_1 - T_2}{C_1 - C_2}, \; D_f = \frac{\rho c_p D}{k_1}\frac{C_1 - C_2}{T_1 - T_2}, (15)$$
$$N_1 = \frac{k}{\rho\nu}, \; N_2 = \frac{\nu_s}{\rho\nu h^2}, \; N_3 = \frac{j}{h^2}, \; Re = \frac{v_0 h}{\nu},$$
$$Pr = \frac{\nu\rho c_p}{k_1}, \; Sc = \frac{\nu}{D^*}, \; Gr = \frac{g\beta_T A h^4}{\nu^2},$$
$$Pe_h = Pr\, Re, \quad Pe_m = Sc\, Re, \quad (16)$$

where Pr is the Prandtl number, Sc is the generalized Schmidt number, λ is the local buoyancy number, N_1 is the coupling parameter and N_2 is the spin-gradient viscosity parameter. In technological processes, the parameters of particular interest are the local Nusselt and Sherwood numbers. These are defined as follows:

$$Nu_x = \frac{q''_{y=-h}\, x}{(T_1 - T_2)k_1} = -\theta'(-1), \quad (17)$$
$$Sh_x = \frac{m''_{y=-h}\, x}{(C_1 - C_2)D^*} = -\phi'(-1). \quad (18)$$

where q'' and m'' are local heat flux and mass flux respectively.

3 Method of solution

Equations (9) - (12) are coupled and highly nonlinear. Various solution methods such as finite difference methods (for example, Al-Azab [39]), perturbation methods as in Abdella and Magpantay [40] and multi-parameter perturbation method (as in Boricic et al. [38]) and elsewhere can be used to solve these equations. In this study we use the homotopy analysis method (HAM) to determine approximate analytical solutions to the system of nonlinear ordinary differential equations (9) - (12). Compared to traditional perturbation methods, the HAM has the advantage that it does not require the existence of a no small or large parameter to give good accuracy. The solutions are validated by solving equations (9) - (12) numerically using the Matlab routine bvp4c. The analytic series solutions to equations (9) - (12) represented as

$$f(\eta) = f_0(\eta) + \sum_{m=1}^{+\infty} f_m(\eta), \quad (19)$$
$$g(\eta) = g_0(\eta) + \sum_{m=1}^{+\infty} g_m(\eta), \quad (20)$$
$$\theta(\eta) = \theta_0(\eta) + \sum_{m=1}^{+\infty} \theta_m(\eta), \quad (21)$$
$$\phi(\eta) = \phi_0(\eta) + \sum_{m=1}^{+\infty} \phi_m(\eta). \quad (22)$$

where $f_m(\eta)$, $g_m(\eta)$, $\theta_m(\eta)$ and $\phi_m(\eta)$ are the m^{th} order deformation equations and the initial approximations

$$f_0(\eta) = (1 + \eta - \eta^2 - \eta^3)/4, \quad (23)$$

$$g_0(\eta) = \frac{1}{2} + \frac{1}{2}\eta, \tag{24}$$

$$\theta_0(\eta) = \frac{1}{2} - \frac{1}{2}\eta, \tag{25}$$

$$\phi_0(\eta) = \frac{1}{2} - \frac{1}{2}\eta, \tag{26}$$

are chosen so as to satisfy the boundary conditions (13) - (14). To give insight into the structure of the solution we present (in the absence of Dufour and Soret effects) the solutions for the velocity $f(\eta)$ and the angular velocity $g(\eta)$ below

$$\begin{aligned} f_1(\eta) &= -\left(\frac{9}{22400}Re\right)\eta^7 - \frac{3Re}{3200}\left(\eta^6 - \eta^5\right) \\ &- \left(\frac{3}{640}Re\right)\eta^4 + \frac{22400}{69}\left(\frac{69}{89600} - Re\right)\eta^3 \\ &+ \frac{3200}{39}\left(Re - \frac{39}{12800}\right)\eta^2 \\ &+ \frac{22400}{39}\left(\frac{39}{89600} - Re\right)\eta \\ &+ \frac{3200}{21}\left(\frac{21}{12800} - Re\right) \end{aligned} \tag{27}$$

$$\begin{aligned} g_1(\eta) &= \frac{1}{160}\left(N_3Re\right)\eta^5 + \frac{1}{48}\left(N_3Re\right)\eta^4 \\ &+ \frac{1}{48}\left(N_3Re + 10N_1\right)\eta^3 + \frac{3}{8}N_1\eta^2 \quad . \end{aligned} \tag{28}$$

4 Convergence of the solutions

The convergence rate and region of the solution series depends on the auxiliary parameters $\hbar_f$, $\hbar_g$, $\hbar_\theta$ and $\hbar_\phi$. To find admissible values of these parameters for which the series solutions (19) - (22) will converge we plot the $\hbar$-curves, graphs of, say, $f''(-1)$, $f''(1)$, $g''(-1)$ and $g'(1)$ versus $\hbar$ as shown in Figures 1 - 2 for different orders of approximation of the series solutions.

The series solutions would converge for those values of $\hbar$ that lie on the horizontal segment of the $\hbar-$curves. For fixed parameter values, the range of admissible values of $\hbar_f$, $\hbar_g$ and $\hbar_\theta$ are such that $-1.5 \le \hbar \le -0.3$. The accuracy of the HAM solutions is determined by comparing the series solutions with the numerical approximations obtained using the inbuilt Matlab bvp4c.

5 Results and Discussions

The system of equations governing the heat and mass transfer in an incompressible micropolar fluid along a porous channel has been solved using the homotopy analysis method and the Matlab bvp4c numerical routine. The effects of the governing fluid parameters

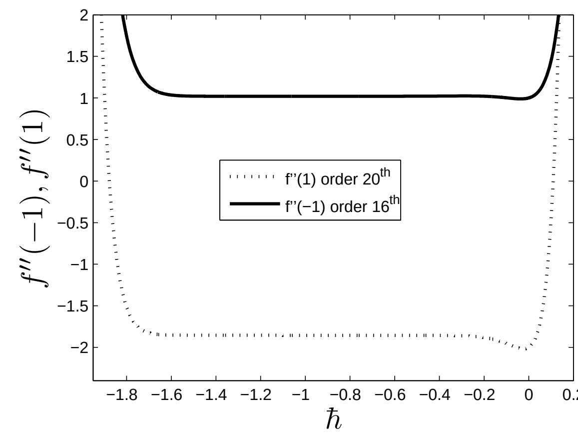

Figure 1: The $\hbar$ curves for the twentieth order HAM solution series when $N_1 = N_2 = N_3 = 1, Re = Pe_h = 1$, $Pe_m = 0.8$, $D_f = S_r = 0$

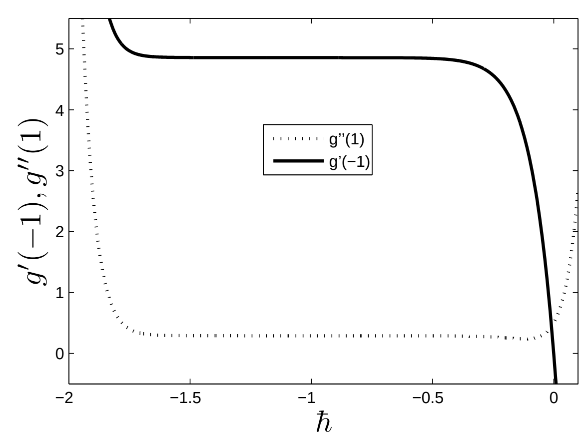

Figure 2: The $\hbar$ curves for $g'(1)$ and $g''(1)$ at the twentieth order HAM solution series when $N_1 = N_2 = N_3 = 1, Re = Pe_h = 1$ and $Pe_m = 0.8$, $D_f = S_r = 0$

Table 1: Effect of the Soret S_r and Dufour D_f numbers on the heat and mass transfer rates when $Pe_h = 1.0$ and $Pe_m = 0.8$. The other parameters are $N_1 = N_2 = N_3 = Re = 1$

S_r	D_f	Nu_x	Sh_x
2.0	0.03	0.26421	0.81762
1.0	0.12	0.26674	0.56626
0.5	0.30	0.29824	0.40619
0.1	0.60	0.37986	0.33580

Table 2: Effect of the Soret S_r and Dufour D_f numbers on the heat and mass transfer rates when $Pe_h = Pe_m = 1.0$. The other parameters are $N_1 = N_2 = N_3 = Re = 1$

S_r	D_f	Nu_x	Sh_x
2.0	0.03	0.26561	0.77499
1.0	0.12	0.27325	0.51578
0.5	0.30	0.31577	0.37325
0.1	0.60	0.41284	0.28422

such as the Reynolds Number Re, the Peclet number Pe, the Dufour and Soret numbers on the velocity, microrotation, temperature and concentration profiles has been determined and shown in Figures 3 - 26.

For heat and mass transfer, the point of primary interest is at the wall when $\eta = -1$. This represents the Nusselt and Sherwood numbers which are proportional to $-\theta'(-1)$ and $-\phi'(-1)$ respectively.

Tables 1 - 2 illustrate the effects of the Dufour and Soret parameters on the heat and mass transfer rates at different Peclet numbers. The Nusselt number increases with the Dufour parameter but decreases with the Soret effect. On the other hand, mass transfer increases with the Soret effect but decreases with Dufour numbers.

Tables 3 - 4 illustrate the effect of the Peclet number on the Nusselt and Sherwood numbers respectively. It is evident that increases in the Peclet number leads to decreases on the Nusselt and Sherwood numbers. This is because increasing Pe decreases the momentum transport in the boundary layer.

Figures 3 - 4 give a comparison of the twentieth order HAM approximations and the numerical results at different Peclet numbers. Two observations can be made; firstly that is evident that at the twentieth order the HAM has sufficiently converged to the numerical solution and the two results are identical, and secondly that in the absence of Dufour and Soret effects, the heat and mass transfer decrease in numerical value with increasing Peclet numbers.

Figures 5 - 6 show the effect of the Reynolds num-

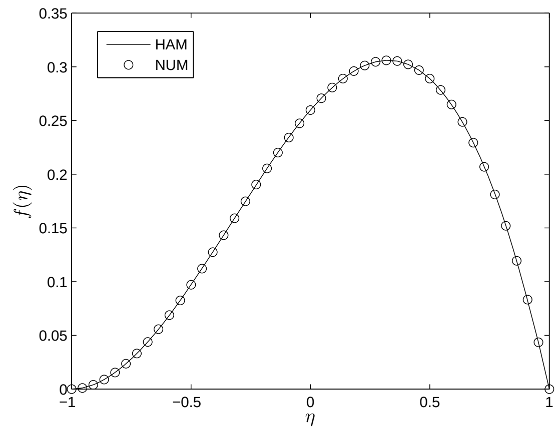

Figure 3: Velocity profiles obtained using the 20^{th} order HAM approximation (—) and the bvp4c numerical routine when $N_1 = N_2 = N_3 = 1,\ Re = Pe_h = 1$ and $Pe_m = 0.8$, $D_f = S_r = 0$

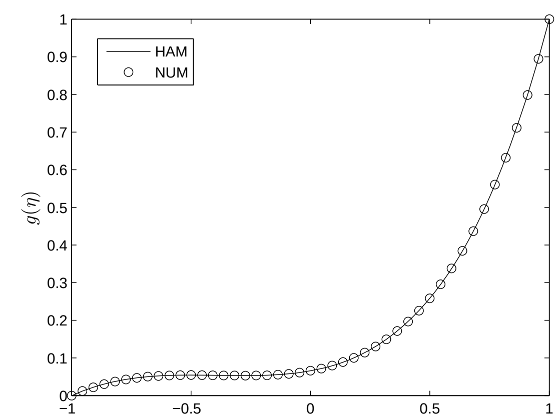

Figure 4: Micro rotation profiles obtained using the 20^{th} order HAM approximation (—) and the bvp4c numerical routine when $N_1 = N_2 = N_3 = 1,\ Re = Pe_h = 1$ and $Pe_m = 0.8$, $D_f = S_r = 0$

Table 3: Effect of the Peclet number Pe_h on $-\theta'(-1)$ for $N_1 = N_2 = 1,\ N_3 = Re = 1$ and $Pe_m = 0.8$, $D_f = S_r = 0$

Pe_h	NUM	11^{th}	18^{th}	20^{th}
0.07	0.48543	0.48573	0.48545	0.48544
0.20	0.45789	0.45883	0.45797	0.45793
0.40	0.41426	0.41635	0.41445	0.41436
0.50	0.39185	0.39460	0.39211	0.39198
1.00	0.27337	0.28046	0.27414	0.27378
2.00	-0.00115	0.02209	0.00207	0.00067
3.00	-0.34059	-0.28380	-0.33056	-0.33448

Table 4: Effect of the Peclet number Pe_m on $-\phi'(-1)$ for $N_1 = N_2 = N_3 = Re = 1$ and $Pe_h = 1$, $D_f = S_r = 0$

Pe_m	NUM	11^{th}	17^{th}	19^{th}
0.00	0.50000	0.50000	0.50000	0.50000
0.10	0.47913	0.47978	0.47922	0.47918
0.20	0.45789	0.45926	0.45809	0.45800
0.50	0.39185	0.39578	0.39248	0.39219
0.80	0.32210	0.32931	0.32333	0.32278
2.00	-0.00115	0.00298	0.00554	0.00286
3.00	-0.34059	-0.14128	-0.14991	-0.15499

ber on the velocity and micro rotation vector. Increasing the Reynolds number leads to a decrease in the velocity and the micro rotation vector. The Reynolds number has little effect on the temperature and concentration fields.

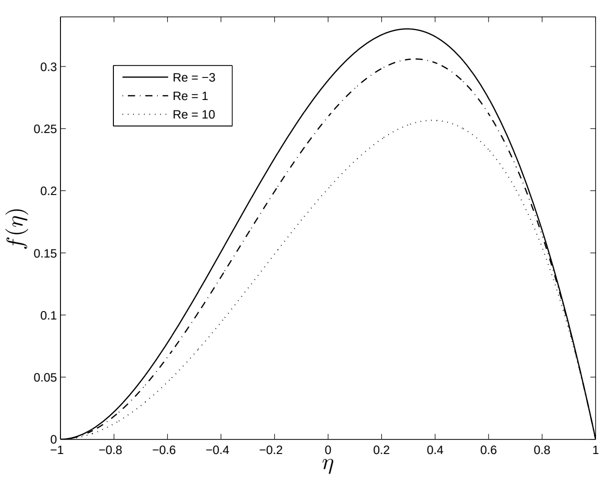

Figure 5: Effect of moderate Reynolds numbers on the velocity profiles when $N_1 = N_2 = N_3 = 1,\ Pe_h = 1$, and $Pe_m = 0.8$, $D_f = S_r = 0$

Figures 7 - 8 show the effects of N_1 on the ve-

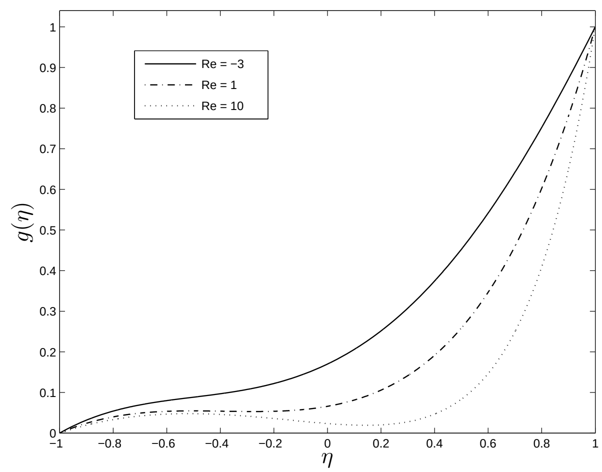

Figure 6: Effect of moderate Reynolds numbers on micro rotation profiles when $N_1 = N_2 = N_3 = 1,\ Pe_h = 1$, and $Pe_m = 0.8$, $D_f = S_r = 0$

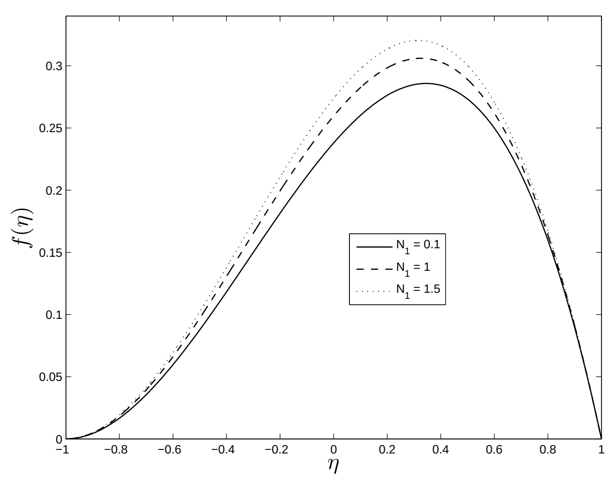

Figure 7: Velocity profiles for various values of N_1 when $N_2 = N_3 = 1,\ Pe_h = 1$, and $Pe_m = 0.8$, $D_f = S_r = 0$

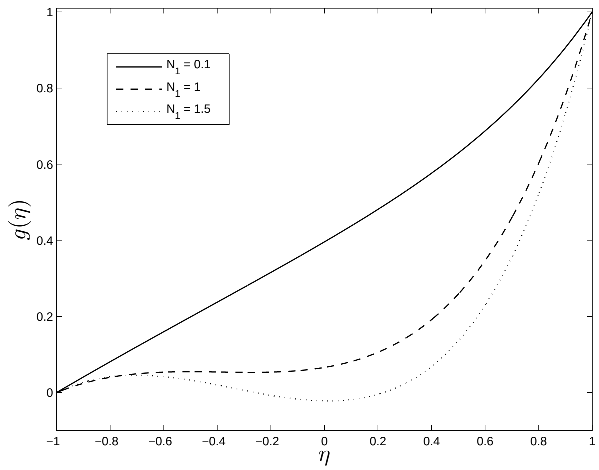

Figure 8: Microrotation profiles for various values of N_1 when $N_2 = N_3 = 1,\ Pe_h = 1$, and $Pe_m = 0.8$, $D_f = S_r = 0$

locity and micro rotation profiles respectively. The velocity increases with increases in N_1, but the microrotation decreases with increasing N_1.

Figures 9 - 10 show the effect of N_2 on the fluid properties when all the other parameters are fixed. The velocity profile decreases with increases in N_2. Similarly, with the range $N_2 \geq 0.7$, the angular velocity increases with N_2. However, when $N_2 < 0.7$ the behavior of the angular velocity is oscillatory and irregular. The parameter N_3 was found to have an effect only on the angular velocity and as shown in Figure 11, increasing N_3 leads to a decrease in the angular velocity.

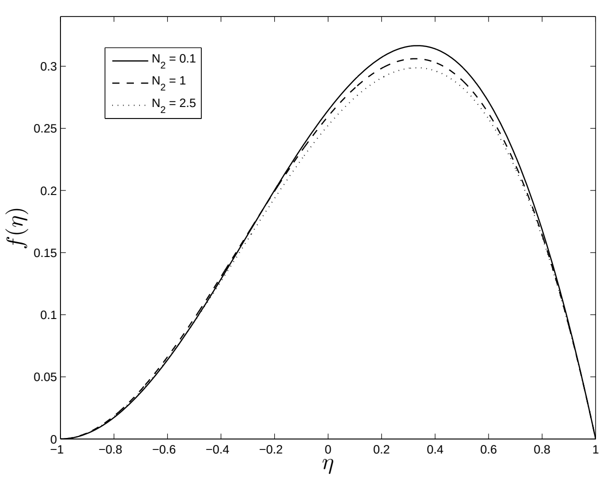

Figure 9: Velocity profiles for various values of N_2 when $N_1 = N_3 = 1,\ Re = Pe_h = 1$, and $Pe_m = 0.8$, $D_f = S_r = 0$

The topographical effect of the Peclet number

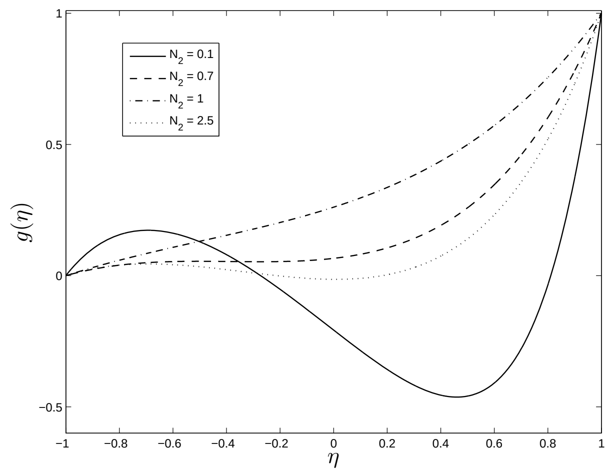

Figure 10: Micro rotation profiles for various values of N_2 when $N_1 = N_3 = 1,\ Re = Pe_h = 1$, and $Pe_m = 0.8$, $D_f = S_r = 0$

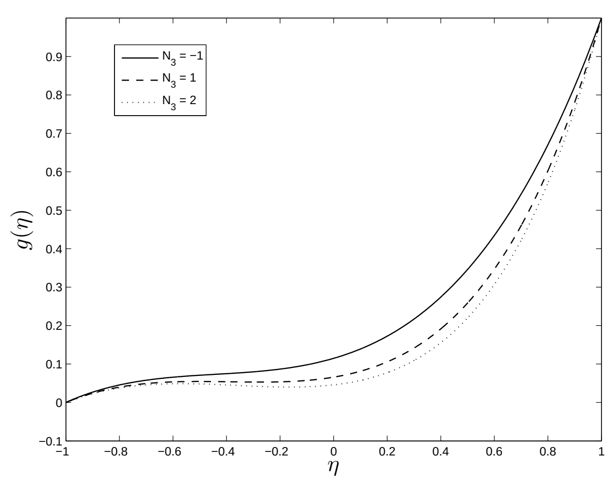

Figure 11: Micro rotation profile for various values of N_3 when $N_1 = N_2 = 1,\ Re = Pe_h = 1$, and $Pe_m = 0.8$, $D_f = S_r = 0$

on the fluid temperature and solute concentration is shown in Figures 12 - 15. In Figure 12 the effect of small Peclet number (restricted to the range $0 \leq Pe \leq 5$) while the effect of moderate Peclet numbers $5 < Pe \leq 13$ is shown in Figure 13. Increasing the Peclet number leads to an increase in the temperature fields with the maximum temperature occurring in the middle of the channel. However, the Peclet number was found to have no effect on the velocity and the microrotation vectors.

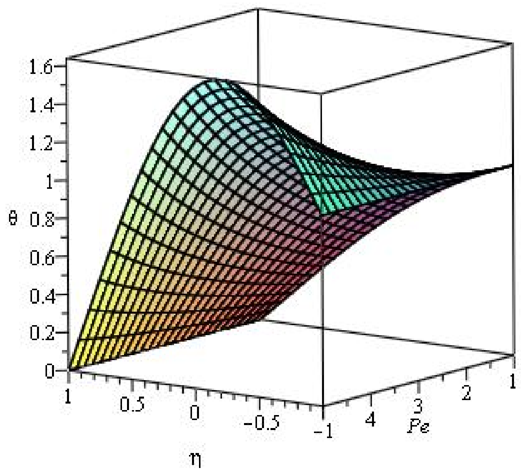

Figure 12: The effect of the Peclet number on the temperature profile shown in 3D when $0 \leq Pe_h = Pe_m = Pe \leq 5$ when $N_1 = N_2 = N_3 = 1$ and $Re = 1$

Figures 14 - 15 show the effect of low to moderate Peclet numbers on the solute concentration. Low Peclet numbers tend to promote high mixing while high Peclet numbers inhibit the mixing. As expected, low Peclet numbers result in low solute concentration while high Peclet numbers result in high solute concentrations.

Figures 16 - 17 represent the temperature profiles for different Soret numbers. The impact of the Soret parameter on the temperature depends on whether $Pe_h > Pe_m$ or $Pe_h < Pe_m$. Thus in Figure 16 where $Pe_h = 2$ and $Pe_m = 9$, the temperature of the fluid decreases with Soret numbers whereas in Figure 17 where $Pe_h = 6$ and $Pe_m = 0.5$, the fluid temperature increases with the Soret parameter. The effect of the Soret parameter on the concentration profiles is shown in Figures 18 - 19 where, again, it is evident that the concentration of the solute either decreases or

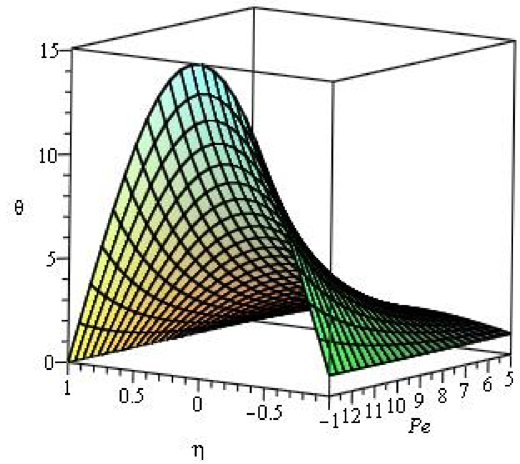

Figure 13: The effect of moderate Peclet numbers ($5 \leq Pe_h = Pe_m = Pe \leq 13$) on the temperature profile in 3D when $N_1 = N_2 = N_3 = 1$ and $Re = 1$

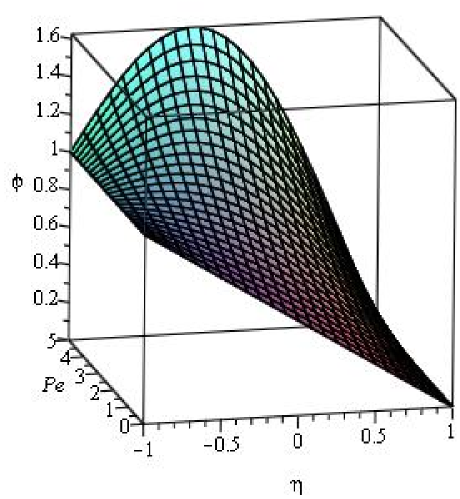

Figure 14: Concentration profile in 3D obtained using the 20^{th} HAM for various values of $0 \leq Pe_h = Pe_m = Pe \leq 5$ when $N_1 = 1,\ N_2 = 1,\ N_3 = 1$ and $Re = 1$

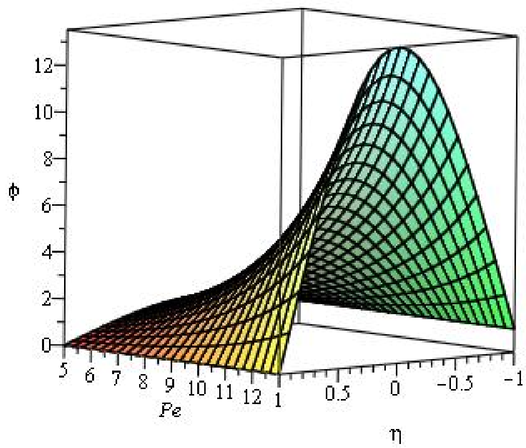

Figure 15: Concentration profile in 3D obtained using the 20th HAM for various values of $5 \leq Pe_h = Pe_m = Pe \leq 13$ when $N_1 = 1,\ N_2 = 1,\ N_3 = 1$ and $Re = 1$

increases with the Soret parameter depending on the relative sizes of the Peclet numbers Pe_h and Pe_m.

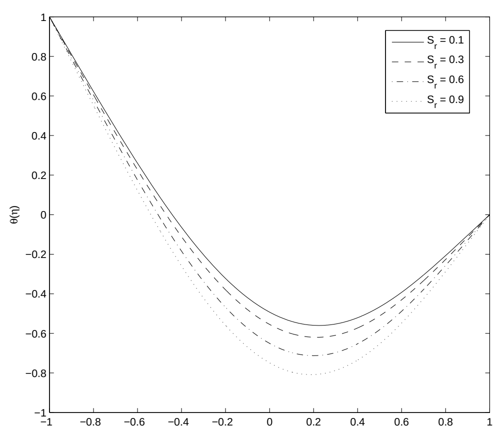

Figure 16: The effect of the Soret number S_r on the temperature profiles when $N_1 = N_2 = N_3 = 1,\ Re = 1,\ Pe_h = 2,\ Pe_m = 9$ and $D_f = 0.3$

Figures 20 - 22 show the effect of the Dufour parameter on the temperature and concentration profiles. The fluid temperature decreases with the Dufour parameter when $Pe_h < Pe_m$. On the other hand, the concentration profiles increase marginally with the

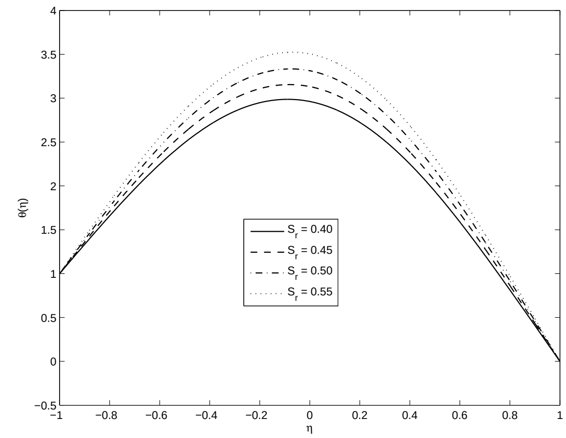

Figure 17: The effect of the Soret number S_r on the temperature profiles when $N_1 = N_2 = N_3 = 1,\ Re = 1,\ Pe_h = 6,\ Pe_m = 0.5$ and $D_f = 0.8$

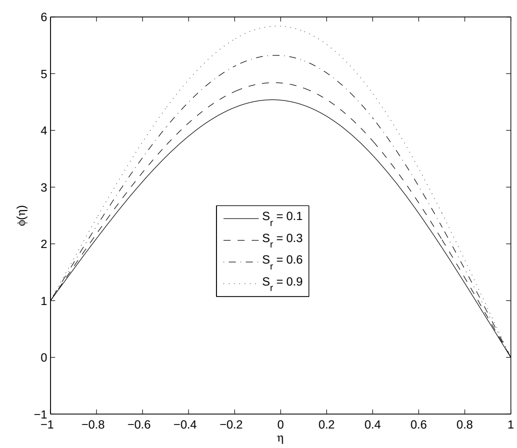

Figure 18: The effect of the Soret number S_r on the concentration profiles when $N_1 = N_2 = N_3 = 1,\ Re = 1,\ Pe_h = 2,\ Pe_m = 9$ and $D_f = 0.3$

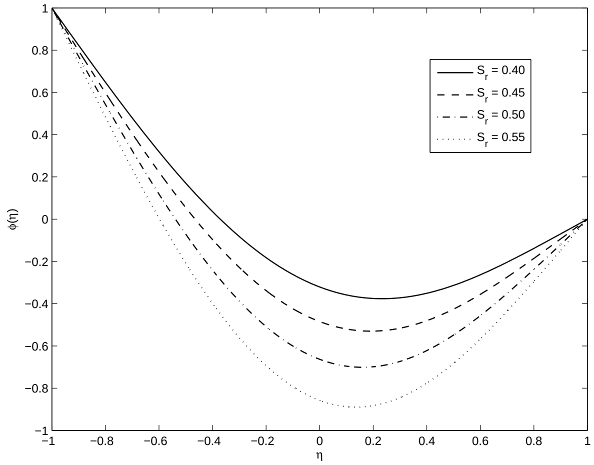

Figure 19: The effect of the Soret number S_r on the concentration profiles when $N_1 = N_2 = N_3 = 1,\ Re = 1,\ Pe_h = 6,\ Pe_m = 0.5$ and $D_f = 0.8$

Dufour parameter when $Pe_h < Pe_m$ but decrease with Dufour parameters when $Pe_h > Pe_m$. An earlier study by Monsour et al. [41] showed that the temperature and concentration profiles decrease with increasing Dufour numbers.

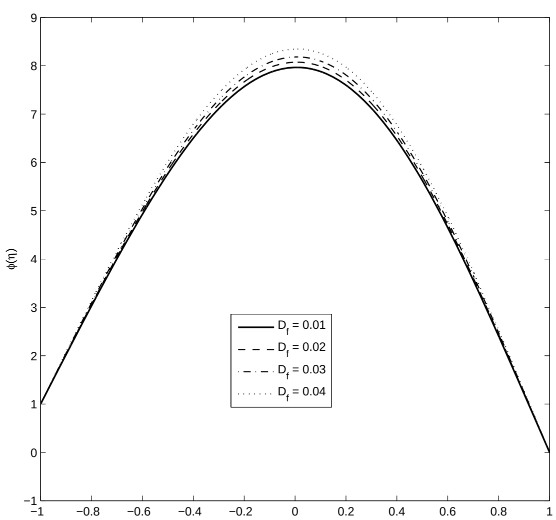

Figure 20: The effect of the Dufour number D_f on the temperature profiles when $N_1 = N_2 = N_3 = 1,\ Re = 1,\ Pe_h = 5,\ Pe_m = 12$ and $S_r = 0.5$

Figures 23 - 26 show the effects of the Dufour and Soret parameters on the heat and mass transfer coefficients. We observe that, as in the study by Cheng [42], as the Dufour number is increased, the local Nusselt number decreases while the local Sherwood number increases. We further deduce that; (i) mass transfer increases with the Dufour parameter for all Soret numbers, and (ii) heat transfer decreases with the Soret

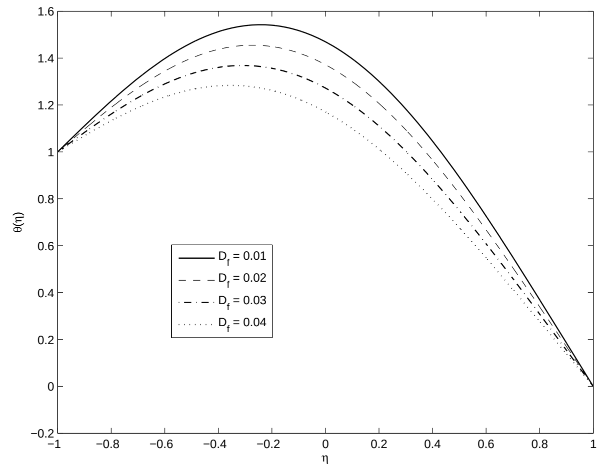

Figure 21: The effect of the Dufour number D_f on the concentration profiles when $N_1 = N_2 = N_3 = 1,\ Pe_h = 5,\ Pe_m = 12$ and $S_r = 0.5$

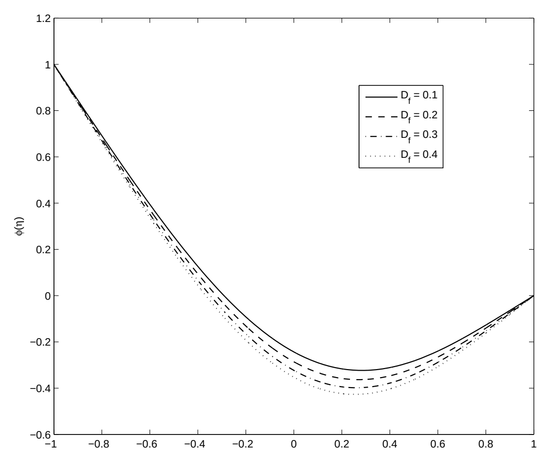

Figure 22: The effect of the Dufour number D_f on the concentration profiles when $N_1 = N_2 = N_3 = 1,\ Re = 1,\ Pe_h = 5,\ Pe_m = 4$ and $S_r = 0.9$

effect for all Dufour numbers.

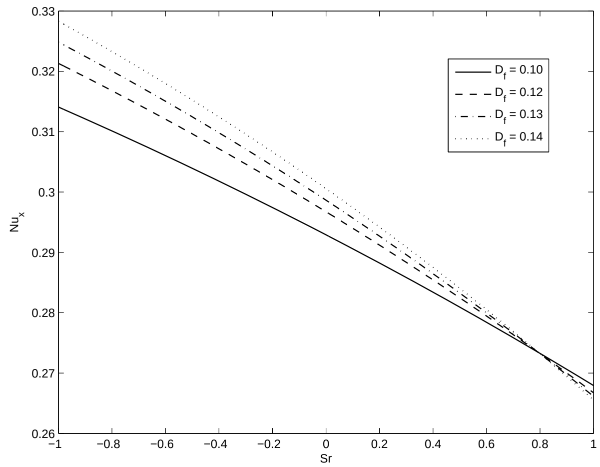

Figure 23: Non-dimensional heat transfer coefficient as a function of S_r at fixed $N_1 = N_2 = N_3 = 1,\ Re = 1,\ Pe_h = 1,\ Pe_m = 0.8$

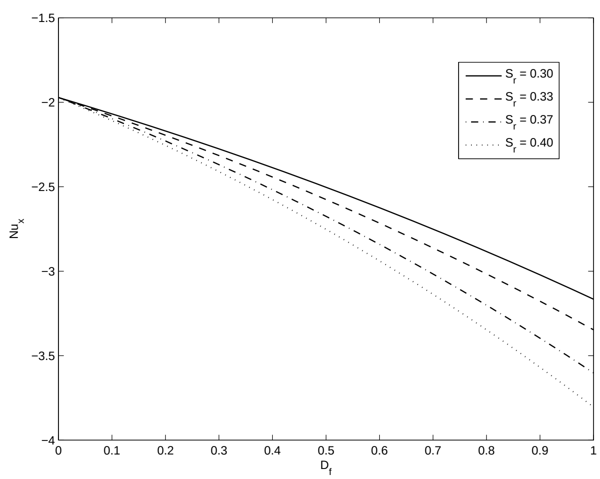

Figure 24: Non-dimensional heat transfer coefficient as a function of D_f at fixed $N_1 = N_2 = N_3 = 1,\ Re = 1,\ Pe_h = 6$ and $Pe_m = 0.5$

6 Conclusion

In this paper we have studied the effects of the Dufour, Soret and Peclet parameters on a the heat and mass transfer on a micropolar fluid through a horizontal channel. The analysis shows that the Soret and Dufour parameters have a significant influence on the thermal and solutal boundary layer profiles. The effect of the Peclet numbers on the fluid properties has been determined. Our analysis shows that;

- the increase or decrease in the boundary layer

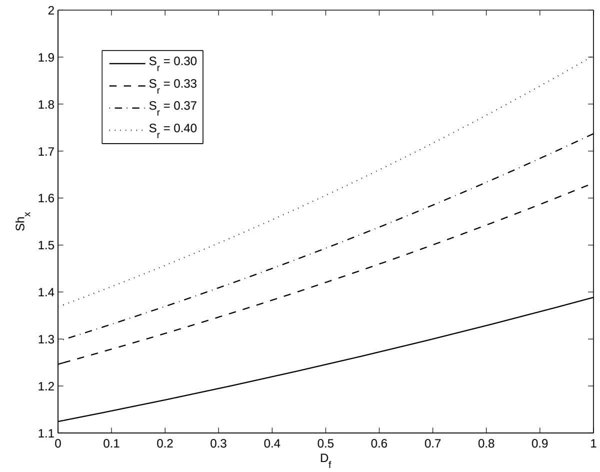

Figure 25: Non-dimensional mass transfer coefficient as a function of D_f at fixed $N_1 = N_2 = N_3 = 1,\ Re = 1,\ Pe_h = 6,\ Pe_m = 0.5$

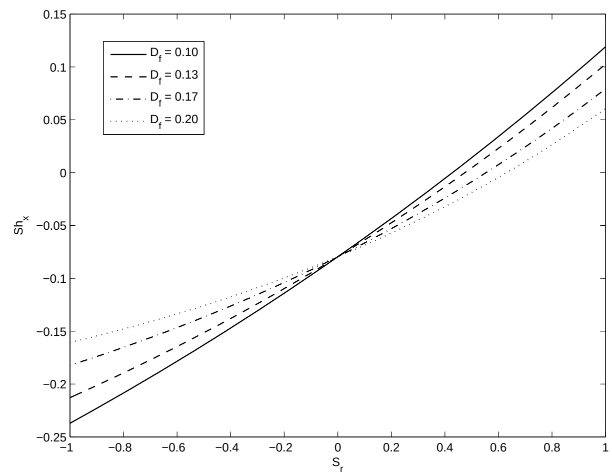

Figure 26: Non-dimensional mass transfer coefficient as a function of S_r at fixed $N_1 = N_2 = N_3 = 1,\ Re = 1,\ Pe_h = 6,\ Pe_m = 0.5$

temperature and concentration is dictated by the relative sizes of Pe_h and Pe_m in the analysis,

- increasing Reynolds numbers reduces both the velocity and micro-rotation profiles,

- the velocity increases with N_1 whereas the micro-rotation vector decreases with N_1.

References

[1] A. C. Eringen, Theory of micropolar fluids, *J. Math. Mech.*, Vol. 16, 1966, pp. 1 - 18.

[2] A. C. Eringen, Theory of thermomicropolar fluids, *J. Math. Anal. Appl.*, Vol. 38, 1972, pp. 480 - 496.

[3] B. Hadimoto and T. Tokioka, Two-dimensional shear flows of linear micropolar fluids, *Int. J. Engi. Sci.*, Vol. 7, 1969, pp. 515 - 522.

[4] F. Lockwood, M. Benchaitra and S. Friberg, Study of polyotropic liquid crystals in viscometric flow and clastohydrodynamic contact, *ASLE Tribology Trans.*, Vol. 30, 1987, pp. 539 - 548.

[5] T. Ariman, M. A. Turk and N. D. Sylvester, Microcontinuum fluid mechanics a review, *Int. J. Eng. Sci.*, Vol. 12, 1974, pp. 273 - 293.

[6] M.-E. M. Khedr, A. J. Chamkha and M. Bayomi, MHD Flow of a Micropolar Fluid past a Stretched Permeable Surface with Heat Generation or Absorption, *Nonlinear Analysis: Modelling and Control*, Vol. 14, 2009, pp. 27 - 40.

[7] J. Peddieson and R. P. Mcnitt, Boundary layer theory for a micropolar fluid, *Recent Adv. Engng. Sci.*, Vol. 5, 1970, pp. 405 - 426.

[8] R. S. Gorla, Heat transfer in micropolar boundary layer flow over a flat plate, *Int. J. Eng. Sci.*, Vol. 21, 1983, pp. 791 - 796.

[9] D. A. S. Rees and A. P. Bassom, The Blasius boundary layer flow of a micropolar fluid, *Int. J. Eng. Sci.*, Vol. 34, 1996, pp. 113 - 124.

[10] N. A. Kelson and A. Desseaux, Effects of surface conditions on flow of a micropolar fluid driven by a porous stretching sheet, *Int. J. Eng. Sci.*, Vol. 39, 2001, pp. 1881 - 1897.

[11] C. Perdikis and A. Raptis, Heat transfer of a micropolar fluid by the presence of radiation, *Heat Mass Transfer*, Vol. 31, 1996, pp. 381 - 382.

[12] A. Raptis, Flow of a micropolar fluid past a continuously moving plate by the presence of radiation, *International Journal of Heat and Mass Transfer*, Vol. 41, 1998, pp. 2865 - 2866.

[13] H. A. M. El-Arabawy, Effect of suction/injection on the flow of a micropolar fluid past a continuously moving plate in the presence of radiation, *Int. J. Heat Mass Tran.*, Vol. 46, 2003, pp. 1471 - 1477.

[14] E. M. Abo-Eldahab and A. F. Ghonaim, Radiation effect on heat transfer of a micropolar fluid through a porous medium, *Appl. Math. Comput.*, Vol. 169, 2005, pp. 500 - 510.

[15] I. A. Hassanien, A. H. Essawy and N. M. Moursy, Natural convection flow of micropolar fluid from a permeable uniform heat flux surface in a porous medium, *Appl. Math. Comput.*, Vol. 152, 2004, pp. 323 - 335.

[16] W. A. Aissa and A. A. Mohammadein, Joule heating effects in a micropolar fluid past a stretching sheet with variable electric conductivity, *J. Comput. Appl. Mech.*, Vol. 6, 2005, pp. 3 - 13.

[17] V. M. Soundalgekar and H. S. Takhar, Flow of a micropolar fluid past a continuously moving plate, *Int. J. Engng. Sci.*, Vol. 21, 1983, pp. 961 - 965.

[18] A. A. Mohammadein and R. S. R. Gorla, Heat transfer in a micropolar fluid over a stretching sheet with viscous dissipation and internal heat generation, *Int. J. Num. Meth. Heat Fluid Flow*, Vol. 11(1), 2001, pp. 50 - 58.

[19] M. M. Rahman and T. Sultana, Radiative Heat Transfer Flow of Micropolar Fluid with Variable Heat Flux in a Porous Medium, *Nonlinear Analysis: Modelling and Control*, Vol. 13, 2008, pp. 71 - 87.

[20] Y. J. Kim and J. -C. Lee, Analytical studies on MHD oscillatory flow of a micropolar fluid over a vertical porous plate, *Surface and Coatings Technology*, Vol. 171, 2002, pp. 187 - 193.

[21] R. C. Sharma and U. Gupta, Thermal convection in micropolar fluids in porous medium, *Int. J. Eng. Sci.*, Vol. 33 no. 13, 1995, pp. 1887 - 1892.

[22] R. Nazar, A. Ishak and I. Pop, Unsteady Boundary Layer Flow over a Stretching Sheet in a Micropolar Fluid, *WSEAS Engineering and Technology*, Vol. 38, 2008, pp. 118 - 122.

[23] Z. Ziabakhsh, G. Domairry and H. Bararnia, Analytical solution of non-Newtonian micropolar fluid flow with uniform suction/ blowing and heat generation, *J. Taiwan Institute of Chemical Engineers*, Vol. 40, 2009, pp. 443 - 451.

[24] R. Muthucumaraswamy and P. Ganesan, Effect of the chemical reaction and injection on flow characteristics in an unsteady upward motion of an isothermal plate, *J. Appl. Mech. Tech. Phys.*, Vol. 42, 2001, pp. 665 - 671.

[25] F. S. Ibrahim, A.M. Elaiw and A. A. Bakr, Effect of the chemical reaction and radiation absorption on the unsteady MHD free convection flow past

a semi-infinite vertical permeable moving plate with heat source and suction, *Comm. Nonlinear Sci. Numer. Simulat.*, Vol. 13, 2008, pp. 1056 - 1066.

[26] R. A. Mohamed and S. M. Abo-Dahab, Influence of chemical reaction and thermal radiation on the heat and mass transfer in MHD micropolar flow over a vertical moving porous plate in a porous medium with heat generation, *International Journal of Thermal Sciences*, Vol. 48, 2009, pp. 1800 - 1813.

[27] Z. Ziabakhsh and G. Domairry, Homotopy analysis solution of Micro-Polar flow in a porous channel with high mass transfer, *Adv. Thoer. App. Mech.*, Vol. 1, 2008, pp. 79 - 94.

[28] M. Sajid, Z. Abbas and T. Hayat, Homotopy analysis for boundary layer flow of a micropolar fluid through a porous channel, *Applied Mathematical Modelling*, Vol. 33, 2009, pp. 4120 - 4125.

[29] P. A. L. Narayana, and P. Sibanda, Soret and Dufour Effects on Free Convection along a Vertical Wavy Surface in a Fluid Saturated Darcy Porous Medium, *International Journal of Heat and Mass Transfer*, Vol. 53, 2010, pp. 3030 - 3034.

[30] A. Mojtabi, M. C. Charrier-Mojtabi, Double diffusive convection in porous media, Handbook of Porous Media, 2nd Edition, 2005.

[31] A. Postelnicu, Influence of a magnetic field on heat and mass transfer by natural convection from vertical surfaces in porous media considering Soret and Dufour effects, *International Journal of Heat and Mass Transfer*, Vol. 47, no. 6-7, 2004, pp. 1467 - 1472.

[32] S. Alam, M. M. Rahman, A. Maleque, and M. Ferdows, Dufour and Soret effects on steady MHD combined free-forced convective and mass transfer flow past a semi-Infinite vertical plate, *Thammasat International Journal of Science and Technology*, Vol. 11, no. 2, 2006, pp. 112.

[33] M. S. Alam and M. M. Rahman, Dufour and Soret effects on mixed convection flow past a vertical porous flat plate with variable suction, *Nonlinear Analysis: Modelling and Control*, Vol. 11, no. 1, 2006, pp. 3 - 12.

[34] M.-C. Li, Y.-W. Tian, and Y.-C. Zhai, Soret and Dufour effects in strongly endothermic chemical reaction system of porous media, *Transactions of Nonferrous Metals Society of China*, Vol. 16, no. 5, 2006, pp. 1200 - 1204.

[35] S. N. Gaikwad, M. S. Malashetty, and K. Rama Prasad, An analytical study of linear and nonlinear double diffusive convection with Soret and Dufour effects in couple stress fluid, *International Journal of Non-Linear Mechanics*, Vol. 42, no. 7, 2007, pp. 903913.

[36] D.A. Nield, A. Bejan, Convection in Porous Media, second ed., Springer-Verlag, New York, 1999.

[37] I. Pop, D.B. Ingham, Convective Heat Transfer, first ed., Elsevier, 2001.

[38] Z. Boricic, D. Nikodijevic, B. Blagojevic, Z. Stamenkovic, Universal solution of unsteady two-dimensional MHD boundary layer on the body with temperature gradient along surface, *WSEAS Transactions on Fluid Mechanics*, Vol. 4, no. 3, 2009, pp. 97 - 106.

[39] T. Al-Azab, Unsteady mixed convection heat and mass transfer past an infinite porous plate with thermophoresis effect, *WSEAS Transcations on Heat and Mass Transfer*, Vol. 4, no.2, 2009, pp. 23 - 33.

[40] K. Abdella, F. Magpantay, Approximate analytic solution for mixed and forced convection heat transfer from an unsteady no-uniform flow past a rotating cylinder, *WSEAS Transcation on Heat and Mass Transfer*, Vol. 2, no. 1, 2007, pp. 6 - 16.

[41] M.A. Mansour, N.F. El-Anssaryb, A.M. Aly, Effects of chemical reaction and thermal stratification on MHD free convective heat and mass transfer over a vertical stretching surface embedded in a porous media considering Soret and Dufour numbers, *Chemical Engineering Journal*, Vol. 145, 2008, pp. 340 - 345.

[42] C. -Y. Cheng, Soret and Dufour effects on natural convection heat and mass transfer from a vertical cone in a porous medium, *International Communications in Heat and Mass Transfer*, Vol. 36, 2009, pp. 1020 - 1024.